Impact of Urbanization on Land Cover Changes and Land Surface Temperature in Iseyin Local Government Area, Oyo State, Nigeria

Adeleke S.O.[1], Moshood F.J.[2,*]

[1] *Department of Surveying and Geo-informatics, University of Lagos, Nigeria*
[2] *Department of Forest Production and Products, University of Ibadan, Nigeria*
**moshoodfarhan@gmail.com*

Date Received: December 05, 2022 Date Accepted: December 30, 2022

Abstract

Urbanization, without any iota of doubt, is one of the leading factors modifying the Earth's surface because it has a significant impact on land cover changes and Land Surface Temperature (LST). This study assessed the impact of urbanization on land cover changes and LST in Iseyin Local Government Area. Landsat images of 22 years duration (2000, 2013, and 2022) and 30 m resolution were used in the study. The result showed that in 2000, vegetation occupied 58538 ha (43%), the built-up areas covered 2535 ha (2%), farmland covered 61248 ha (45%), rocky/hilly areas accounted for 3226 ha (2.4%), water bodies accounted for 431.17 ha (0.3%) while bare land covered 8642 equivalent to 6.42% of the area. In 2013, the built-up area occupied 3.4% (4577 ha), water body covered 0.21% (281 ha), vegetation covered 35% (48136 ha), farmland covered 48% (64352 ha), bare land covered 11% (15944 ha) while rocky/hilly area covered 1.02% (1376 ha). In 2022, built-up areas covered 6393 ha (4.8%), water bodies, vegetation and farmland covered 515 ha, 33819 ha, and 75999 ha respectively while bare land and rocky/hilly areas also covered 14346 ha and 3594 ha respectively. The LST result showed a mean temperature value of about 32^{o}C, 27^{o}C and 29^{o}C in 2000, 2013, and 2022 respectively. The study concludes that urbanization has largely affected the land cover types in Iseyin LGA and increased the LST between 2000 and 2022. The study has therefore provided a scientific reference to policymakers to develop effective and sustainable policies in Iseyin LGA.

Keywords*:* Urbanization, Land Cover Changes, Iseyin, Land Surface Temperature, Landsat images

1. Introduction

According to the United Nations (2018), about 68% of the human population will be living in urban areas by 2050 due to urbanization. This will affect the land cover and land surface temperature. The need to develop infrastructures that will curb the giant needs of the populace leads to rapid changes in vegetation, water and soils will be replaced with artificial structures such as buildings, roads, and other erections (Fortuniak, 2009; Gill et al., 2007).

Through urbanization, natural land covers such as vegetation will be converted to artificial land use types such as residential, recreational, industrial and transportation land uses. These man-made land use types make urban landscapes patchy and complex which will in turn affect the habitability of towns (Alberti and Marzluff, 2004). The surface temperatures were said to have been increasing globally as a consequence of anthropogenic factors (Imhoff et al., 2010; Partha et al., 2019).

Several studies have shown the vital role played by vegetation in the reduction of the impact of urban heating in urban areas (Amusa et al., 2022; Chen et al., 2013; Zhibin et al., 2015). One

ISSN 2235-9362 Online ©2022 University of Sri Jayewardenepura

of the effects of urbanization on the environment is what is known as Urban Heat Island (UHI). According to Voogt and Oke (2003), UHI refers to the difference in surface temperature between rural and urban environments such that the urban environment is warmer. This phenomenon occurs because of the structures that absorb and re-emit the sun's heat. With the rising impact of UHI on human health, it is important to assess the effect of urbanization on Land Surface Temperature (Burkart et al., 2011; Igun and Williams, 2018).

Like other developing climes, there has been rapid urbanization in Iseyin Local Government Area recently. In 2005, the estimated population according to the United Nations was approximately 236,000 (Oyewole, 2021). Although there is no recent census in Nigeria to support the recent population in Iseyin LGA, visual observation and satellite images have shown that the population has increased beyond what it used to be. It is believed that urbanization impacts land cover changes and land surface temperature. This work, therefore, studied the impact of urbanization on land cover changes and land surface temperature in Iseyin LGA between 2000 and 2022.

2. Materials and Methods

2.1 Study area

The study was carried out in Iseyin LGA of Oyo State, Nigeria (Figure 1). Iseyin is one of the LGAs that constitutes what is known as Oke-Ogun region of Oyo State (Adeyemo, 2016). It is geographically situated on latitudes $3^o1'0''$ E and $7^o50'0''$ N and longitudes $3^o1'0''$ and $3^o40'0''$ N and covers an area of about 134, 668 ha. It is bounded in the North by Itesiwaju LGA, in the south by Ibarapa East LGA, in the west by Kajola LGA, and in the east by Oyo West and Afijio LGAs (Ikemenanwa et al., 2020). It has an average annual rainfall of about 1149 mm, a mean relative humidity of about 72% annually, and an annual mean temperature of 24.4 °C (Obi-Egbedi et al., 2022).

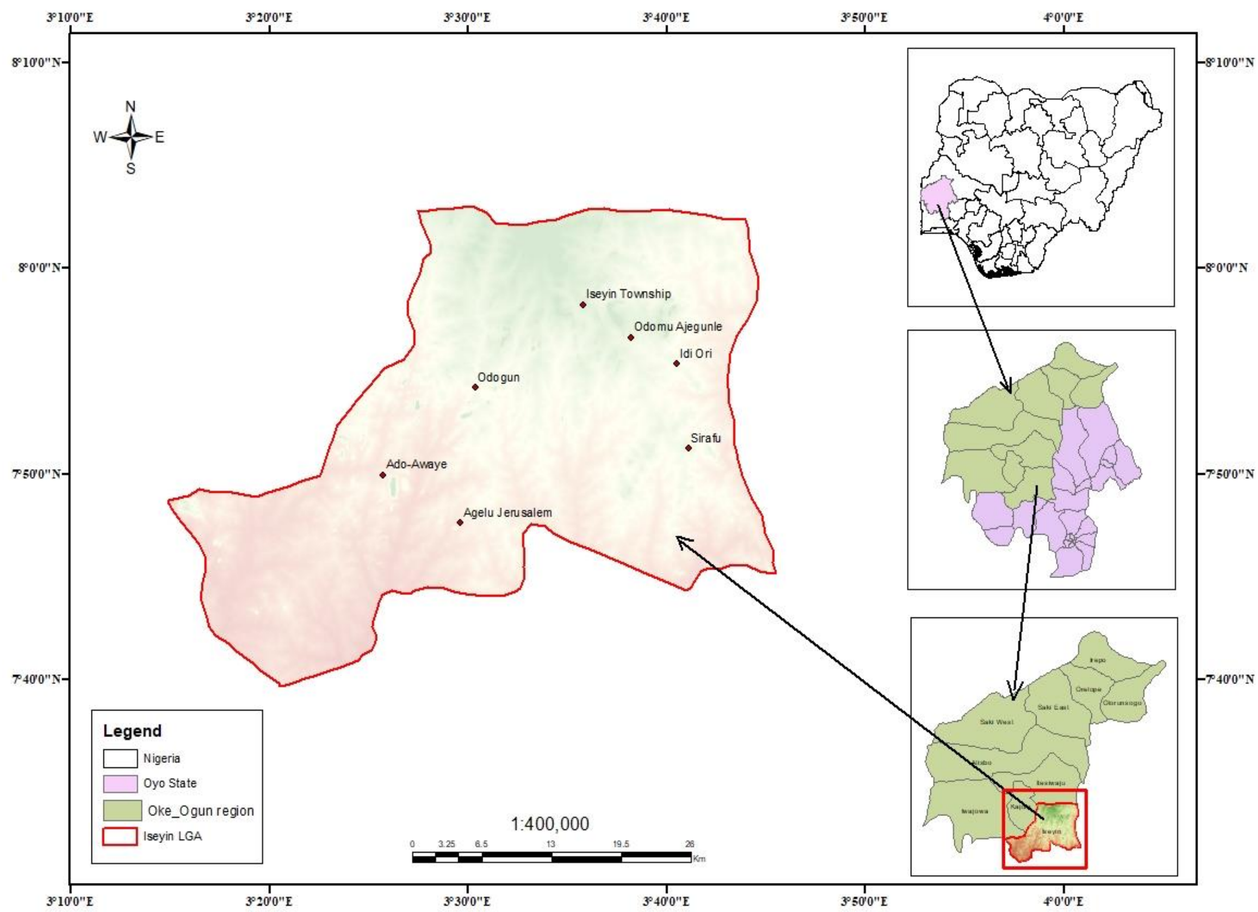

Figure 1: Map of Iseyin Local Government Area (inset map of Nigeria and map of Oyo State)

2.2 Data acquisition

Landsat images were downloaded from the United State Geological Survey (USGS) website using the part and row values (191/055) covering Iseyin LGA. Images with less than 10% cloud cover were downloaded for this study. The characteristics of the images are presented in Table 1. All downloaded images fall into approximately the same season.

Table 1: Landsat imagery dataset details

Year	Sensor	Scene ID	Path / Row	Resolution
2000	ETM	LE71910552000037EDC00	191 / 055	30m
2013	OLI / TIRS	LC81910552013352LGN01	191 / 055	30m
2022	OLI / TIRS	LC81910552022025LGN00	191 / 055	30m

2.3 Image analysis

Image importing

Based on the nature of the software used for this research, there is a need for the downloaded images to be converted into a well-recognized format for easy processing, and the importing features of the software helped in executing the conversion process.

Image layer stacking

Image layer stacking is a pre-process operation to put together all the imported Landsat bands converted from TIFF to IMG format. This layer stacking process helps proper band combination for colour visualization before classification. All eleven (11) bands were stacked together for Landsat 8 and nine (9) bands for Landsat 7.

Image classification

Image classification is sorting different pixels into a finite number of individual classes or categories of data based on the data fields. This was achieved using colour differencing. The supervised image classification scheme was employed for this research work.

2.4 Trend analysis

The land cover changes in the study area were calculated using equation (1).

Land Cover Changes = $(L2 - L1)$ (1)

2.5 Rate of change

$R_t = \{(L_2 - L_1) \times \frac{1}{L1 * t}\} \times 100$ (2)

Where: R_t = rate of change, L_1 (ha) = present year, L_2 (ha) = base year and t (year) = periodic interval

2.6 Accuracy assessment

This process involves ground-truthing which helped in locating the actual features physically and collecting coordinate points reading for each of the desired classification classes and then comparing the collected coordinates to the classified image for accuracy.

Sensitivity (Producer's accuracy) $= \frac{a}{a+c}$ (3)

Positive predictive power (User's accuracy) $= \frac{a}{a+b}$ (4)

Overall accuracy $= \frac{\text{Total Number of Correct Samples}}{\text{Total Number of Samples}} \times 100$ (5)

Kappa coefficient (K) $= \frac{N\sum_{i=1}^{r} xii - \sum_{i=1}^{r}(xi + X_{XI+1})}{N^2 - \sum_{i=1}^{r}(xi + X_{XI+1})}$ (6)

Where: a = number of times a classification agreed with the observed value; b = number of times a point was classified as "a" when it was observed to not be "a"; c = number of times a point was not classified as "a" when it was observed to be "a"; d = number of times a point was not classified as "a" when it was not observed to be "a"; r = number of rows and columns in the confusion matrix; N = total number of ground-truthed points (pixels); Xii = observation in row i and column i; Xi = marginal total of row i, and Xi+1 = marginal total of column i.

2.7 Normalized Difference Vegetation Index (NDVI)

$$NDVI = \frac{NIR - RED}{NIR + RED} \quad (7)$$

Where: NIR = Near Infrared and RED = Red band

2.8 Top of Atmospheric (TOA) Spectral Radiance

$$TOA\ (L) = ML * Qcal + AL \quad (8)$$

Where: M_L = Band-specific multiplicative rescaling factor; Q_{cal} = corresponds to band 10 and A_L = Band-specific additive rescaling factor (Isa et al., 2016)

2.9 Top of Atmospheric to Brightness Temperature Conversion

$$BT = \left(\frac{K2}{1}\left(ln\left(\frac{K1}{1}L\right) + 1\right)\right) - 273.15 \quad (9)$$

Where: K_1 = Band-specific thermal conversion and K_2 = Band-specific thermal conversion constant (Srivastava et al., 2022)

2.10 Land Surface Emissivity (LSE)

$$E = 0.004 \times PV + 0.986 \quad (10)$$

Where: E = Land Surface Emissivity and 0.986 correspond to a correction value of the equation (Isa et al., 2016).

2.11 Proportion of vegetation

$$PV = \left(\frac{NDVI - NDVI\ min}{NDVI\ \mathrm{max} - NDVI\ min}\right)^2 \quad (11)$$

Where: PV = Proportion of Vegetation, NDVI = DN values from NDVI image, $NDVI_{min}$ = Minimum DN values from NDVI image, and $NDVI_{max}$ = Maximum DN values from NDVI image (Srivastava et al., 2022).

2.12 Land Surface Temperature (LST)

$$LST = \frac{BT}{1 + (\lambda \times BT / C2) \times \ln(E)} \quad (12)$$

Where: BT = Top of Atmosphere Brightness Temperature (^oC), λ = Wavelength of emitted radiance, E = Land Surface Emissivity, C2 = h × c / s (1.4388×10^{-2} mK) = 14388mK, h = Plank's Constant (1.38×10^{-2}Js), s = Boltzmann Constant (1.38×10^{-23}JK) and c = Velocity of light (2.998×10^8 m/s) (Isa et al., 2016).

2.13 Land use/ land cover classes

The distinct land use/ land cover types in the study area are presented in Table 2

Table 2: Land use/land cover types in the study area

Land Use Land Cover	Description
Built-up	This indicates areas covered with houses and other buildings that increase over time
Vegetation	These are areas covered with trees, shrubs, and closed-canopy forests. It also includes plantation of trees and cash crops
Farm/Agric Land	Areas where food or cash crops are grown for agricultural purposes.
Rocky/Hilly Area	These areas have high relief occupying features such as rocks and hills or sand domes
Water	The water bodies are the areas occupied by river and stream flow
Bare Land	Areas with open land with no use

3. Results

3.1 Spatial extent of land cover between 2000 and 2022

The result of the spatial extent of the different land use types in Iseyin Local Government Area is presented in Table 3. In 2000, vegetation occupied about 58538 ha (43.50%), the built-up area covered approximately 2535 ha (1.88%), farmland covered 61248 ha (45.48%), rocky/hilly area accounted for 3226 ha (2.40%), water bodies accounted for about 431 ha (0.32%) while bare land covered about 8642 (6.42% of the area). In 2013, the built-up area covered 3.40% (4577 ha), water body covered 0.21% (281 ha), vegetation covered 35.74% (48136 ha), farmland covered 47.79% (64352 ha), bare land covered 11.84% (15944 ha) while rocky/hilly area covered 1.02% (1376 ha). In 2022, built-up areas covered 6393 ha (4.75%), water bodies, vegetation and farmland covered 515 ha, 33819 ha, and 75999 ha respectively, Bare land and rocky/hilly areas also covered 14346.0 ha and 3594 ha in the same year (Table 3). The land cover changes map is shown in Figure 2.

Table 3: Spatial extent of land use types in Iseyin Local Government Area

LULC	2000 Area (ha)	Area (%)	2013 Area (ha)	Area (%)	2022 Area (ha)	Area (%)
Built-up	2535.84	1.88	4577.42	3.40	6393.53	4.75
Water	431.17	0.32	281.72	0.21	515.28	0.38
Vegetation	58583.60	43.50	48136.10	35.74	33819.90	25.11
Farm/Agric Land	61248.60	45.48	64352.30	47.79	75999.30	56.43
Bare Land	8642.43	6.42	15944.50	11.84	14346.00	10.65
Rocky/Hilly Land	3226.79	2.40	1376.39	1.02	3594.40	2.67
Total	134668.43	100.00	134668.43	100.00	134668.41	100.00

3.2 Accuracy assessment result

The overall accuracy of the classification for 2000, 2013, and 2022 was 91.80%, 94.53%, and 91.02%, respectively. The Kappa statistics for 2000, 2013, and 2022 were 0.87, 0.92, and 0.87, respectively. The producer's accuracy ranged between 42.86% and 72.00% in 2000, 33.33% and 100.00% in 2013, and 78.05% and 91.67% in 2022. The user's accuracy in 2000 ranged between 75.32% and 88.14%, 88.45% and 100.00% in 2013, and 78.05% and 91.67% in 2022 (Table 4).

Table 4: Accuracy assessment for the different land use types in Iseyin LGA

	2000		2013		2022	
LULC	PA (%)	UA (%)	PA (%)	UA (%)	PA (%)	UA (%)
Built-up Area	72.00	75.32	100	100	73.33	91.67
Vegetation	89.66	88.14	88.00	88.45	87.84	84.42
Farm/Bare Land	91.94	81.43	94.81	90.12	82.05	78.05

Water bodies	30.80	80.35	33.33	100	-	-
Rocky/Hilly Land	42.86	78.50	83.33	100	81.82	90.00
Overall Accuracy	91.80%		94.53%		91.02%	
Kappa Statistics	0.87		0.92		0.87	

PA – Producer's Accuracy; UA – User's Accuracy

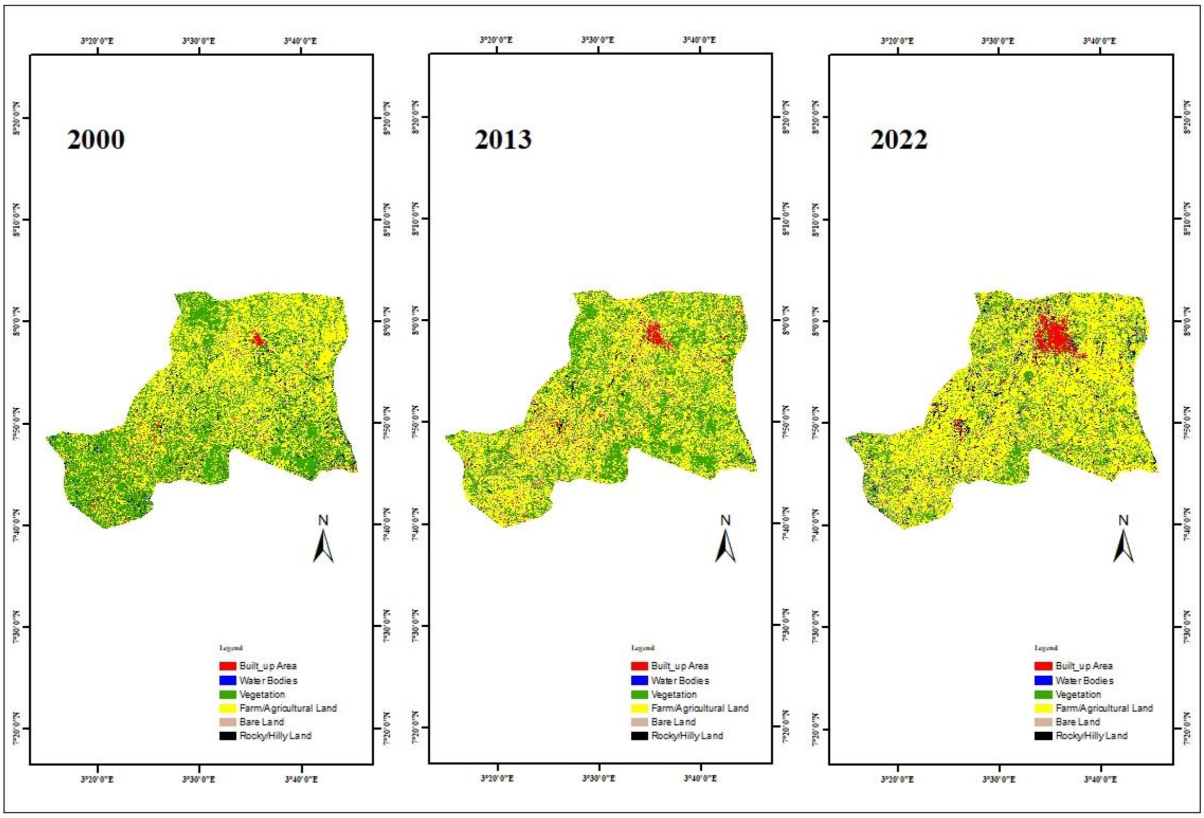

Figure 2: Land Use Cover Map in Iseyin LGA in 2000, 2013 and 2022

3.2 Land surface temperature

Figure 3 presents the land surface temperature (LST) for Iseyin LGA in 2000, 2013, and 2022. In 2000, the minimum LST was 25.53 ^{o}C, the maximum was 48.93 ^{o}C and the mean was 31.74 ^{o}C. The LST result for 2013 showed that there was a decrease in temperature. The maximum, minimum, and mean temperatures were 37.13 ^{o}C, 22.05 ^{o}C, and 27.55 ^{o}C respectively. In 2022, the minimum, maximum, and mean temperatures were 24.08 ^{o}C, 54.21 ^{o}C, and 29.48 ^{o}C respectively. The LST map is shown in Figure 4.

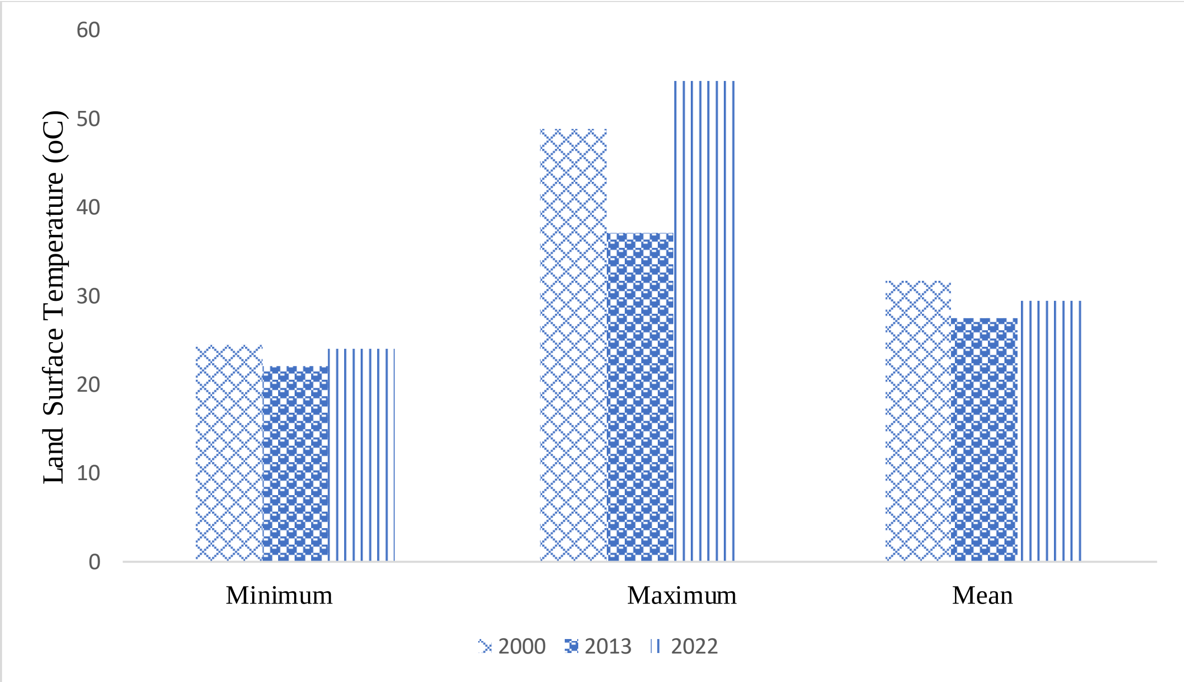

Figure 3: Land Surface Temperature in Iseyin LGA in 2000, 2013 and 2022

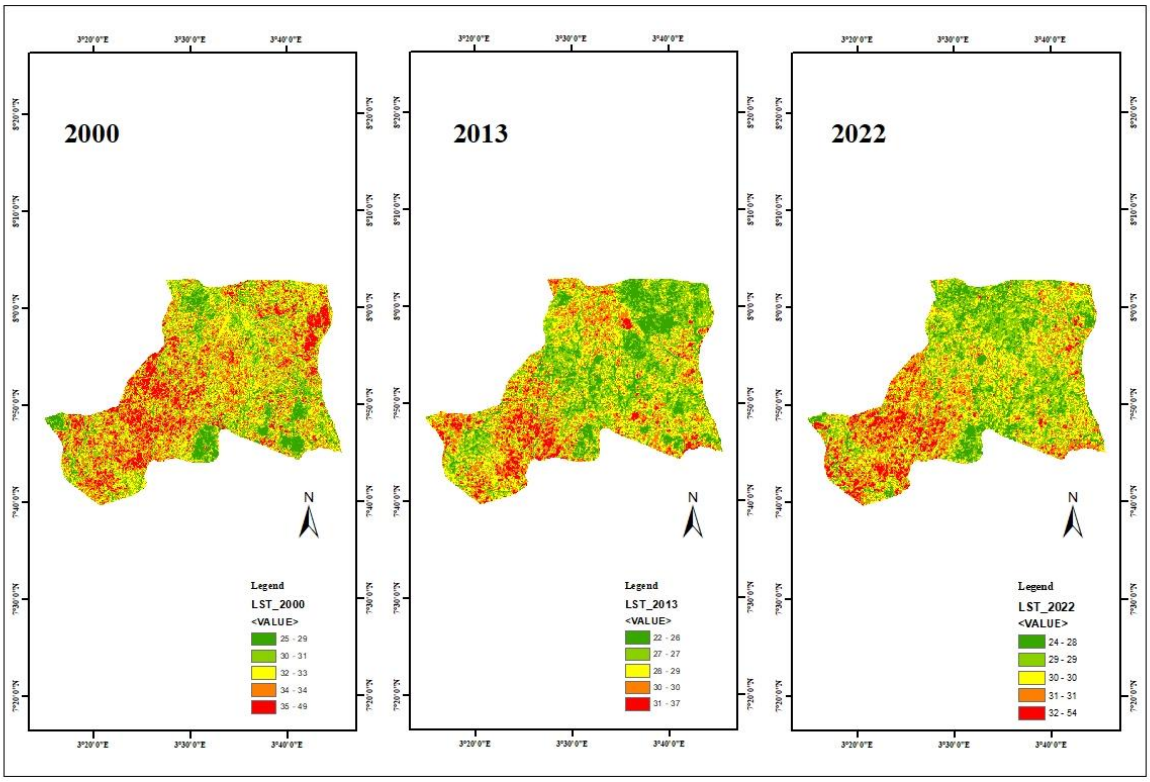

Figure 4: LST map for Iseyin LGA in 2000, 2013 and 2022

4. Discussion

The study revealed the effect of urbanization on land cover changes and land surface temperature in the study area. Our result showed that built-up increased from 2535.84 ha (1.88%) in 2000 to 6393.53 ha (4.75%) in 2022. It also showed that vegetation decreased from 58583.60 ha (43.50%) in 2000 to 33819.90 ha (25.11%) in 2022. On the other hand, farmland increased from 45.48% to 56.43% in 2022. The rapid urban development in Iseyin LGA resulted in the expansion of buildings and the reduction in vegetation. It was necessary to increase the residential building and road networks to cater for the rapid increase in population. Farmland also increased in size probably to meet the food demand of the increasing population. This result agrees with Mbaya et al. (2019) in Gombe metropolis, Hussain et al. (2020) in the district of Multan, and Hussain et al. (2022) in Southern Punjab, Pakistan.

Although no census was conducted in Nigeria from 2007 till 2022, however, the population of Iseyin in 2000 was approximately 220,000 while the population in 2022 was over 450,000 based on the projection of the Nigerian Population Commission (NPC, 2011). The population increase further corroborates the findings of the study. When the population increases in a community, the construction of houses, roads, and other infrastructure increases which will in turn engender the removal of vegetation and extraction of freshwater from the environment (Koko et al., 2021).

One of the consequences of urban expansion is the increase in land surface temperature. The maximum temperature recorded in 2000 was 48.93 ^{o}C. It however increased to 54.21 ^{o}C in 2022. Urbanization often increases temperature because the materials used in construction absorb heat compared to the natural environment. Le et al. (2021) observed higher LST values in the rapidly urbanized Ho Chi Minh City in Vietnam. They noted that LST usually increases when natural environments such as vegetation and water bodies are replaced with non-transpiring surfaces such as metals, stones, and concrete. Fonseka et al. (2019) also observed an increase in LST in Colombo Metropolitan Area, Sri Lanka.

Another major effect of urbanization is Urban Heat Island (UHI). It has been noted that UHI is caused by the removal of natural vegetation and the increase in infrastructures that trap solar energy during the day and release it in form of heat at night (Quattrochi et al., 2000). Amusa et al. (2022) studied the effect of tree canopy cover on an urban heat island in Ilorin metropolis and concluded that trees are useful in reducing the ambient temperature. Vegetation that should rather help absorb surface temperature decreased by 18.39% between 2000 and 2022 in the study area while built-up areas increased by 2.87%.

5. Conclusion

In this study, the impact of urbanization on land cover changes and LST was assessed in Iseyin LGA, Oyo State, Nigeria. The study showed that urbanization has modified the land cover types and increased the LST in the study area. Built-up areas and farmlands increased by 2.87% and 10.85% respectively while vegetation was reduced by 18.39% between 2000 and 2022. The study also recorded up to a 5.28 ℃ difference in the maximum temperature recorded between 2000 and 2022. Although urbanization is important because of the growing world population. However, the land surface temperature can be managed by incorporating certain features in the urban centers. It is recommended that policymakers should focus on planting trees in every urban centre to help absorb heat and reduce the ambient temperature.

References

Adeyemo, O.O. 2016. Operational performance of Ikere-Gorge dam in Iseyin Local Government Area of Oyo State, South-western Nigeria. *International Journal of Advanced Academic Research* 2(8), 8: 19-28.

Alberti, M. and Marzluff, J. 2004. Ecological resilience in urban ecosystems: linking urban patterns to ecological and human function. *Urban Ecosyst*em 7: 241-265

Amiri, R., Weng, Q., Alimohammadi, A. and Alavipanah, S.K. 2009. Spatial–temporal dynamics of land surface temperature in relation to fractional vegetation cover and land use/cover in the Tabriz urban area, Iran. *Remote Sensing of Environment* 113: 2606-2617.

Amusa, T.O., Adebayo, R.A., Moshood, F.J. and Ibrahim, T.M. 2022. Effect of tree canopy cover on Urban Heat Island in Ilorin metropolis, Kwara State, North-central, Nigeria. *Agriculture and Forestry* Journal 6(2): 86-93.

Burkart, K., Schneider, A., Breitner, S., Khan, M.H., Krämer, A. and Endlicher, W. 2011. The effect of atmospheric thermal conditions and urban thermal pollution on all cause and cardiovascular mortality in Bangladesh. *Environmental Pollut*ion 159: 2035-2043

Chen, D., Wang, X., Khoo, Y.B., Thatcher, M., Lin, B.B., Ren, Z. and Barnett, G. 2013. Assessment of urban heat island and mitigation by urban green coverage. *In Mitigating climate change (Springer Berlin Heidelberg)* pp. 247-257.

Fonseka, H.P.U., Zhang, H., Sun, Y., Su, H., Lin, H. and Lin, Y. 2019. Urbanization and its impacts on Land Surface Temperature in Colombo Metropolitan Area, Sri Lanka, from 1988 to 2016. *Remote Sensing* 957(11): 1-19.

Fortuniak, K. 2009. Global environmental change and urban climate in Central European cities. International Conference on Climate Change. The environmental and socio-economic response in the southern Baltic region, University of Szczecin, Poland, 25-28 May 2009. Conference Proceedings. Wyd. International BALTEX Secretariat, Publication, 42: 65-66.

Gill, S.E., Handley, J.F., Ennos, A.R and Pauleit, S., 2007. Adapting cities for climate change: the role of the green infrastructure. *Built Environment* 33(1): 115-133.

Hussain, S., Mubeen, M., Ahmad, A., Majeed, H., Qaisrani, S.A., Hammad, H.M., Amjad, M., Ahmad, I., Fahad, S., Ahmad, N. and Nasim, W. 2022. Assessment of land use/land cover changes and its effect on land surface temperature using remote sensing techniques in Southern Punjab, Pakistan. *Environmental Science and Pollution Research* https://doi.org/10.1007/s11356-022-21650-8.

Hussain, S., Mubeen, M., Akram, W., Ahmad, A., Habib-ur-Rahman, M., Ghafar, A. and Nasim, W. 2020. Study of land cover/land use changes using RS and GIS: a case study of Multan district, Pakistan. Environmental Monitoring and Assessment 192(1): 2 https://doi.org/10.1007/ s10661-019-7959-1.

Igun, E. and Williams, M. 2018. Impact of urban land cover change on land surface temperature. *Global Journal of Environmental Science and Management* 4(1): 47-58.

Ikemenanwa, S.C., Olajide O.A. and Ajayi, O.E 2020. An assessment of the effects of female participation in cassava: adding value for Africa (C: AVA) women empowerement project, with Iseyin Local Government Area of Oyo State, Nigeria, as case study. *Ibadan Journal of Gender Studies* 3 and 4: 167-184.

Imhoff, M.L., Zhang, P., Wolfe, R.E. and Bounoua, L. 2010. Remote sensing of the urban heat island effect across biomes in the continental USA. *Remote Sensing of Environment* 114: 504-513.

Isa, Z., Baba, I.I. and Ayuba, Z. 2016. Estimation of land surface temperature of Kaduna metropolis, Nigeria using Landsat images. *Science World Journal* 11(3): 36-42.

Koko, A.F., Wu, Y., Abubakar, G.A., Alabsi, A.A.N., Hamed, R., Bello, M. 2021. Thirty years of land use/land cover changes and their impact on urban climate: A study of Kano metropolis, Nigeria. *Land* 10: 1106.

Le, T.T.H., Nguyen, V.T., Pham, T.L., Tong, T.H.A., La, P.H. 2021. Impacts of urban land cover change on Land Surface Temperature distribution in Ho Chi Minh City, Vietnam. *Journal of the Korean Society of Surveying, Geodesy, Photogrammetry and Cartography* 39(2): 113-122.

Mbaya, L.A., Abu, G.O., Makadi, Y.C. and Umar, D.M. 2019. Effect of urbanization on land use land cover in Gombe metropolis. *British Journal of Earth Sciences Research* 7(2): 53-61.

National Population Commission (NPC) 2011. Nigeria National Census: Population distribution by sex, state, LGAs and senatorial districts. Abuja, Nigeria.

Nwilo, P.C., Olayinka, D.N., Obiefuna, J., Atagbaza, A.O. and Adzandeh, A.E. 2012. Determination of Land Surface Temperature (LST) and Potential Urban Heat Island effect in parts of Lagos State using satellite imageries. *Futy Journal of the Environment* 7(1): 19-33.

Obi-Egbedi, S.O., Osanyinlusi, O.I. and Adekunle, O.B. 2022. Does contract farming really matter in cassava farms productivity in Iseyin Local Government Area, Oyo State, Nigeria? *Agricultura Tropica et Subtropica* 55: 65-73.

Oyewole, M.F. 2021. Factors influencing instability within rural households in Iseyin Local Government Area, Oyo State, Nigeria. *Journal of Home Economics Research* 28(2): 84-95.

Partha, P.G., Vinoj, V., Swain, D., Roberts, G., Dash, J. and Tripathy, S. 2019. Land use and land cover change effect on surface temperature over Eastern India. *Scientific Reports* 9: 8859.

Quattrochi, D., Luvall, J., Rickman, D., Estes, M., Layman, C., Howell, B. 2000. A decision support information system for urban landscape management using thermal infrared data. *Photogrammetric Engineering and remote Sensing* 66(10): 1195-1207.

Sharma, R., Ghosh, A., and Joshi, P.K. 2013. Spatio-temporal footprints of urbanization in Surat, the Diamond City of India (1990–2009). *Environmental Monitoring and Assessment* 185: 3313-3325.

Srivastava, N., Saini, S. and Shukla, S. 2022. Land surface temperature and its correlation with vegetation cover using Landsat data: a study of Gorakhpur, Uttar Pradesh. *International Research Journal of Engineering and Technology* 9(4): 810-818.

United Nations, 2018. 2018 revision of world urbanization. https://www.un.org/development/desa/en/news/population/2018-revision-of-world-urbanization-prospects.html

Voogt, J.A., Oke, T.R. 2003. Thermal remote sensing of urban climates. *Remote Sensing of Environment* 86: 370-384.

World Bank, 2010. World development report for 2010. Development and climate change. Washington D.C: World Bank.

Zhibin, R., Haifeng, Z., Xingyuan, H., Dan, Z. and Xingyang, Y. 2015. Estimation of the relationship between urban vegetation configuration and land surface temperature with remote sensing. *Journal of the Indian Society of Remote Sensing* 43: 89-100.